sustainability

MDPI

Article

Chemical Modification of Commercial Fabrics by Photoinduced Grafting Tannic Acid to Produce Antioxidant and Antibacterial Textiles

Julie Fouilloux [1], Samir Abbad Andaloussi [2], Valérie Langlois [1], Lasâad Dammak [1] and Estelle Renard [1,*]

[1] Institut de Chimie et des Matériaux Paris-Est (ICMPE), Université Paris-Est (UPEC), UMR 7182, CNRS, 2–8 Rue Henri Dunant, 94320 Thiais, France; julie.fouilloux@u-pec.fr (J.F.); langlois@u-pec.fr (V.L.); dammak@u-pec.fr (L.D.)

[2] Laboratoire Eau, Environnement, Systèmes Urbains (LEESU), UMR-MA 102, Université Paris-Est Créteil (UPEC), 61 Avenue Général de Gaulle, 94010 Crétesil Cedex, France; abbad@u-pec.fr

* Correspondence: e.renard@u-pec.fr

Abstract: The goal of this study was to provide antioxidant and antibacterial properties to different types of fabrics via tannic acid (TA) covalent grafting. To that extent, TA was first methacrylated using glycidylmethacrylate. TA derivatives were characterized using infrared spectroscopy and ^{1}H NMR to assess the degree of acrylation. Antioxidant and antibacterial properties of TA were preserved after chemical modification. The coating process was studied using infrared spectroscopy (IR), weight gain, and radical scavenging activity (*RSA*) measurements. To covalently bond TA to raw polypropylene (PP) and PP coated with chitosan, photoinduced grafting was performed. The process was optimized and resulted in fabrics with enough tannic acid to provide strong antioxidant activity, with *RSA* ranging at 95%. The antibacterial activity was assessed against *E. coli* and *S. aureus*, the main strains responsible for nosocomial infections. Results revealed a substantial reduction of bacterial contamination for PP samples coated with chitosan, with stronger activity against *E. coli*, attributed to hydrophobic repellence. This study highlights the benefits of using tannic acid to obtain antioxidant and antibacterial fabrics.

Keywords: tannic acid; antioxidant; antibacterial; chitosan; glycidylmethacrylate; polypropylene fibers

Citation: Fouilloux, J.; Abbad Andaloussi, S.; Langlois, V.; Dammak, L.; Renard, E. Chemical Modification of Commercial Fabrics by Photoinduced Grafting Tannic Acid to Produce Antioxidant and Antibacterial Textiles. *Sustainability* **2024**, *16*, 4352. https://doi.org/10.3390/su16114352

Academic Editor: Vita Di Stefano

Received: 28 March 2024
Revised: 14 May 2024
Accepted: 16 May 2024
Published: 22 May 2024

1. Introduction

An increasing need for functional textiles has grown over the last decades in the textile industry. Fiber coating has attracted a lot of interest in many fields of applications, such as fashion and sports [1], military [2], health care [3], geotextile [4], protective clothing [5], and automotive sectors. And especially, a strong appeal has thrived in the medical fields of drug release [6], wound dressing [7], and tissue engineering [8]. At first, the goal was to provide individual properties. But currently, researchers focus on the combination of properties through multifunctional smart textiles with simultaneous antimicrobial, antioxidant, anti-inflammatory, UV protection, flame retardancy properties, and so on. This can be performed by using macromolecules with various functionalities and reactivities.

In the meantime, growing concerns over the development of environmentally friendly and sustainable processes in industrial chemistry have led to an increase in the use of natural feedstocks. In this context, a rising interest in polyphenols has been observed due to their broad spectrum of chemical properties and molecular structure. Among those polyphenols, tannic acid (TA) has gained a lot of interest in biomedical research. This natural polyphenol can be found in a wide range of plants and food products [9]. Its complex structure made of various catechol and pyrogallol groups imparts numerous chemical properties such as: excellent water solubility, biocompatibility [10], biodegradability [11], strong adhesiveness [12], metal-chelating properties [13], being a

molecular stabilizer [14], being able to create supramolecular interactions [15], having bacterial [16,17], antioxidant [18–20], antiviral [21,22] and anti-inflammation [23,24] properties, as well as broad absorption across UV regions. Along with its wide availability, it is low cost and harmless for the environment.

Antioxidant agents can counteract free radicals and thus prevent the damage they can cause, such as oxidative stress [25]. An increasing number of scientists agree that oxidative stress plays an important role in wound healing [26]. This stress can lead to cell and tissue damage, impeding wound healing. To that extent, it is crucial to develop bioactive dressings and wound-healing isolation materials with antioxidant properties [27].

In the meantime, growing concerns are expressed in the medical environment due to the spread of nosocomial infections such as *Escherichia coli* (*E. coli*) and *Staphylococcus aureus* (*S. aureus*), for instance, via indirect contamination through contact with contaminated surfaces. Thus, the development of antibacterial finishes for medical textiles is increasing [28].

Tannic acid can be adsorbed onto natural fibers such as silk [29,30], cellulose [31], or coton [32,33] thanks to physical interactions such as hydrogen bonding. Numerous studies have been carried out on the chemical modification of polysaccharides, the most abundant family of biobased polymers. Chemical functionalization of cellulose has been successful despite its low reactivity and low solubility [34,35]. However, these processes cannot be transposed in the case of inert fibers such as polypropylene (PP), which are widely used in disposable personal protective equipment in the medical fields. However, PP fibers could be coated with hydrogen bonding polymers such as chitosan, an antibacterial [36–40] polymer derived from aquaculture waste, which will then interact with TA [41]. Another strategy to coat PP fibers with TA would consist of modifying TA reactivity by grafting photopolymerizable functions to covalently graft this derivative onto PP fibers.

To overcome these challenges, tannic acid derivatives were synthesized by a ring opening reaction of a mono epoxide bearing a methacrylate function. The structure and the degree of acrylation (DA) of those derivatives were measured by 1H NMR and infrared spectroscopy (IR). Their antioxidant properties were confirmed by the DPPH (2,2-diphenyl-1-picrylhydrazyl) radical scavenging activity method. Methacrylated derivatives were then used to coat two different types of fibers: inert fibers such as PP and fibers with reactive functions, such as PP fibers coated with chitosan, to take advantage of hydrogen bonding and antibacterial properties. The coating process of TA relied on the photoinduced grafting of methacrylated tannic acid under UV irradiation using a photoinitiator. Modified PP fibers were characterized by IR spectroscopy, gravimetry, and their antioxidant activity was quantified using the DPPH test. The antibacterial efficacy of optimized samples was studied against both bacteria (*E. coli* and *S. aureus*) for samples coated with chitosan.

2. Materials and Methods

2.1. Materials

Tannic acid (TA) was acquired from Thermo Scientific. Glycidylmethacrylate (GMA), chitosan extracts from shrimp with a hydrolysis rate of 87% (characterized by ^{1}H NMR), tris(hydroxymethyl)amino-methane (TRIS HNO_3), 2,2-dimethoxy-2-phenylacetophenone (DMPA, Irgacure 651), and 2,2diphenyl-1-picrylhydrazyl (DPPH) were supplied from Sigma-Aldrich. Triphenylphosphine (TPP) was provided by ACROS. Glacial acetic acid, HCl, ethanol, n-butyl acetate, and methanol were purchased from Carlo Erba. Polypropylene (PP) mats were obtained from filtering devices FFP3 (EN149:2001+A1:2009) SUP AIR facemask. Only the outer layer was used. The chitosan solutions were deposited in aerosol form using an airbrush (RM 250 purchased from MLD PRODUCTS and equipped with a mini air compressor AS-200).

2.2. Synthesis of Methacrylated Tannic Acid

Methacrylated tannic acid was prepared by grafting glycidylmethacrylate (Figure 1). A total of 4.5 g of tannic acid and 96 mg of TPP were dissolved in 36 mL of butyl acetate under an

inert atmosphere and constant stirring. Glycidylmethacrylate was added at two molar ratios, either 10 eq. (3.36 mL, [GMA] = 154 gL^{-1}) or 5 eq. (1.68 mL, [GMA] = 49 gL^{-1}), respectively named TA_{acr}10eq and TA_{acr}5eq. The mixture was left to react for 48 h at 95 °C. The solvent was evaporated to recover the modified tannic acid. The yield of the reaction was calculated as follows:

$$Yield = \frac{m_{exp}}{m_{TA}\left(1 + n_{eq}\frac{M_{GMA}}{M_{TA}}\right)} \times 100 \quad (1)$$

where m_{exp} is the mass of the product (methacrylated tannic acid), m_{TA} is the mass of tannic acid, n_{eq} is the number of molar equivalents (5 or 10) of GMA per tannic acid, and M_{GMA} and M_{TA} are the molecular masses of, respectively, glycidylmethacrylate and tannic acid.

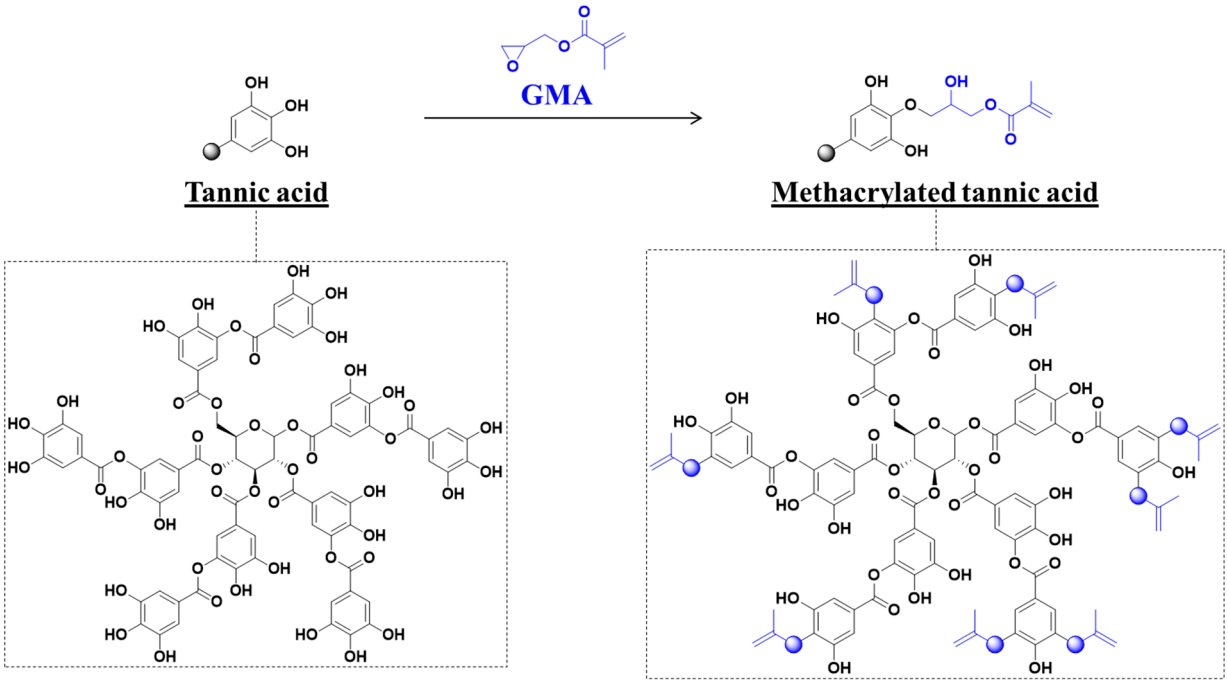

Figure 1. Grafting reaction of methacrylate functions on tannic acid.

2.3. Surface Treatment of Fabric

The process has been previously optimized in our group [42]. PP fabrics (1.5 × 1.5 cm) were coated with chitosan using an airbrush placed at 20 cm from the target. Chitosan was deposited on each side of the PP fiber mat by vaporization (2.5 mL [chitosan] = 15 $g.L^{-1}$ in 1% acetic acid). The chitosan was then immobilized by chemical cross-linking in the presence of oxidized tannic acid as a cross-linking agent. The cross-linking conditions were as follows: 0.1 g of tannic acid was solubilized in 60 mL of TRIS HNO_3 buffer (0.1 M, pH 8.5), stirred for 3 h at 60 °C under an air bubble, and the pH was continuously adjusted to 8.5. After rinsing with distilled water, the tissues were air-dried to a constant mass. This procedure was repeated a second time. The uncross-linked chitosan was removed by rinsing in 5 mL of 1% acetic acid for 24 h.

Photoinduced Chemical Grafting of Methacrylated Tannic Acid

Fabric samples were immersed in 1 mL of a solution of TA_{acr}10eq (100 $g.L^{-1}$) and DMPA (3% wt.) in ethanol. Samples were kept under agitation for 3 h at room temperature. They were then extracted and irradiated under UV light for 300 s for each face with a mercury xenon (180 $mW.cm^{-2}$) lightning cure LC8 (L8251) lamp (Hamamatsu). The distance between the lamp and the sample was 11 cm. Samples were then rinsed in water, washed in 20 mL of ethanol, and dried at 40 °C until constant mass.

The two step process is represented in Figure 2.

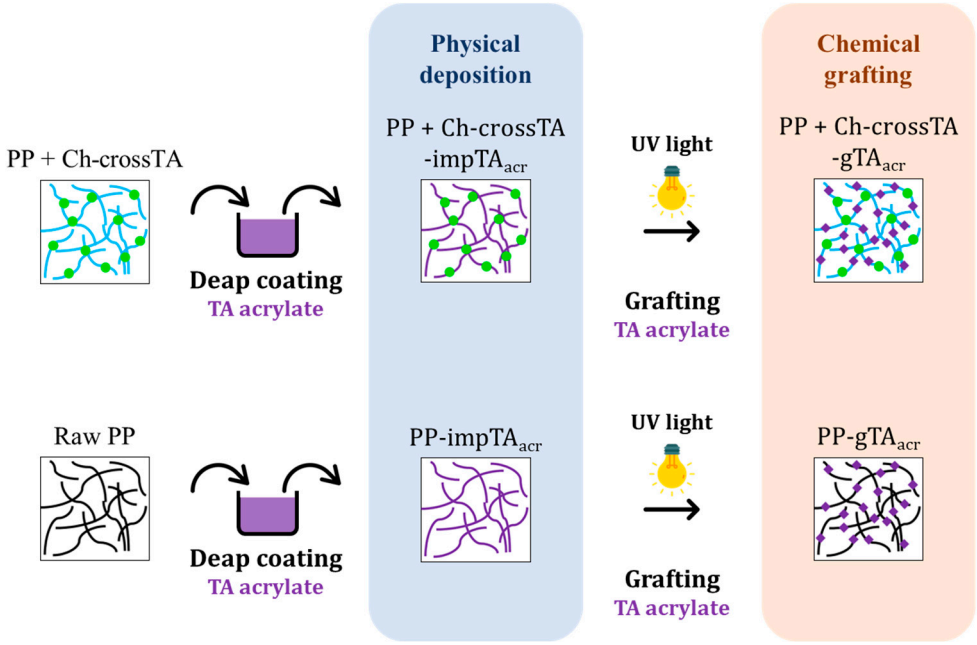

Figure 2. Schematic representation of the two steps process to functionalize fabrics with methacrylated tannic acid.

An additional study was carried out to ensure that the physical impregnation of tannic acid on the surface of the chitosan-modified tissues was insufficient to immobilize a significant quantity of tannic acid on the fabrics. Fabrics were coated by immersion in a solution of TA_{acr}10eq at 100 g.L^1 in ethanol for 3 h at room temperature under stirring. The two types of fabrics used were inert fibers (raw PP) and fibers coated with chitosan (PP fibers are coated with chitosan, which is physically immobilized around the fibers by cross-linking with tannic acid [42]). Before being washed, samples were weighed, and the weight gain associated with it was 42–43% for both fabrics. After ethanol washing, the weight gain drops to 0% for PP fibers and to 4% for the PP coated with cross-linked chitosan. However, based on weight gain measurements, the amount of TA deposited may not be sufficient to provide antibacterial properties.

2.4. Methods

2.4.1. Mass Fraction Determined by Gravimetry

At each step of the process, weight gain was calculated as follows:

$$Weight\ gain(\%) = \frac{m - m_{raw}}{m_{raw}} \times 100 \quad (2)$$

where m is the mass of the functionalized sample, m_{raw} is the initial sample mass before grafting.

2.4.2. Fourier Transform Infrared (FTIR) Spectroscopy

A Bruker Tensor 27 spectrometer equipped with an ATR apparatus was used to acquire Fourier transform infrared (FTIR) spectra with a wavenumber ranging from 4000 to 400 cm^{-1}. A resolution of 4 cm^{-1} with 32 scans accumulated was set, and spectra were recorded in triplicate on each side of each sample. Qualitative characterization of the reactions was ensured by defining different ratios:

$$R_{acr} = \frac{h_{814}}{h_{870}};\ R_{g1} = \frac{h_{1710}}{h_{1375}};\ R_{g2} = \frac{h_{814}}{h_{1375}} \quad (3)$$

where:

h_{1710}: height of C=O stretching band of tannic acid at 1710 cm^{-1}
h_{1375}: height of the CH_3 deformation vibration of PP at 1375 cm^{-1}
h_{870}: height of a C–H vibration of the benzene ring band of TA at 870 cm^{-1}
h_{814}: height of $=CH_2$ twisting vibration of methacrylate band of GMA at 814 cm^{-1}

2.4.3. ^{1}H NMR Spectroscopy

The degree of acrylation (*DA*) of TA was calculated using ^{1}H NMR spectra (400 MHz) performed with a Bruker AII 400 M spectrometer. Methacrylated tannic acid samples were dissolved in DMSO-d6, and experiments were achieved at 25 °C with 64 scans.

$$DA = 20 \times \frac{I_h}{I_a} \quad (4)$$

where I_a is the integral of the massif between 8.0 and 6.7 ppm due to aromatic hydrogens (20 in total in raw tannic acid) and I_h is the signal of the methine hydrogen of methacrylated units at 3.7 ppm.

2.4.4. DPPH Test

Radical scavenging activity (*RSA*) of tannic acid and its derivatives as well as coated fabrics was quantified by measuring the discoloration of 2,2-diphenyl-1-picrylhydrazyl (DPPH) at λ_{max} = 517 nm. This method is based on the reaction of stable free radicals. The DPPH test measures the free radical scavenging capacity of molecules in a model system (organic solvent, room temperature). It measures the ability of an antioxidant (AH, usually phenolic compounds) to reduce the chemical radical DPPH (2,2-diphenyl-1-picrylhydrazyl) by hydrogen transfer. The initially violet DPPH is transformed into the pale-yellow DPPH-H. DPPH reduction is measured at 517 nm (λmax DPPH). The reaction depends on the nature of the antioxidant, and the amount of DPPH-H formed depends on the concentration of the antioxidant. Samples weighing around 10 mg were immersed and kept at room temperature in the dark for 1 h, in 3 mL of DPPH in methanol (0.1 mM). Absorbance was measured at 517 nm using a Varian Cary Bio UV–Visible spectrophotometer. The decrease in absorbance at 517 nm allowed us to calculate the *RSA* as follows:

$$RSA(\%) = \left(\left(A_{ref} - A_s\right)/A_{ref}\right) \times 100 \quad (5)$$

where A_{ref} is the absorbance of the DPPH solution (0.1 mM) and A_s is the absorbance of the DPPH solution (0.1 mM) with 10 mg of samples at 517 nm.

2.4.5. Antibacterial Assays

In vitro measurements were carried out using suspensions of two types of bacteria (*E. coli* (ATCC25922) or *S. aureus* (ATCC6538)). The bacteria are pre-cultured in nutrient medium (Luria Bertani broth) for 24 h at 37 °C.

The antibacterial activity of raw reagents was evaluated in liquid media. To that end, a 96-well plate was prepared by dispensing:

- 180 µL of Luria Bertani (LB) broth,
- 10 µL of TA, TA_{acr}5eq or TA_{acr}10eq solution (100, 10 and 1 $g.L^{-1}$) in DMSO,
- 10 µL of bacterial suspension (concentration of 10^6 $CFU.mL^{-1}$).

The plate was incubated for 16 h at 37 °C. The absorbance at 600 nm of the solutions was measured every 30 min using a UV–visible spectrophotometer.

The antibacterial activity of coated fabrics was assessed using bacterial suspensions according to a procedure developed and validated by our group. The procedure involves bringing the sample into contact with a bacterial suspension. After an optimized contact time of 1 h, adherent bacteria were eliminated. We evaluated the antibacterial activity of the support based on its ability to inhibit the colonization of bacteria on the surface [43,44].

Samples were dipped for 3 h and incubated at 37 °C in bacterial solutions, whose concentrations were set at 10^6 CFU.mL^{-1}. Each experiment was conducted in 4 replicates. Bacteria that did not adhere to the support were removed by successive washing (×7) with sterile saline (NaCl 0.9 w/v), followed by a sonication step (3 mL of NaCl 0.9 w/v for 5 mn). The solutions are then diluted in cascades (concentrations ranging from 10^{-1} to 10^{-5}). From every solution, 100 µL was drop-deposited on Petri dishes, followed by the addition of PCA (Plate Count Agar) bacterial culture media. Colonies were counted after 48 h incubation at 37 °C.

The results were compared using the statistical test as the least significant difference method (LSD) of Fisher.

3. Results and Discussion

3.1. Tannic Acid Methacrylation and Characterization

Tannic acid is known to be a strong antioxidant [18,45] and can be used for antibacterial purposes [16,17,21,45]. Its reactive phenols allow grafting reactions onto other reactive functions such as acids (esterification) [46], alcohols (o-alkylation) [47], coupling with amines [48], and various nucleophilic substitutions. However, raw tannic acid is not polymerizable, making it difficult to coat inert supports. To this end, methacrylated functions were grafted to ensure their polymerization through the support. The methacrylation reaction consisted of a ring-opening reaction of a mono epoxide (glycidylmethacrylate) by tannic acid phenols catalyzed by triphenylphosphine [49]. The number of methacrylated functions per tannic acid was fixed to 5 and 10 to study the impact of the number of methacrylate units per tannic acid on the grafting reaction.

Synthesized methacrylated tannic acids were characterized by infrared Figure 3) and ^{1}H NMR spectroscopy (Figure 4). The degree of methacrylation and the yield of the reaction are presented in Table 1. The FTIR spectra of tannic acid display several characteristic peaks, such as a large massif of the O–H stretching and hydrogen bonding vibrations at around 3300 cm^{-1}, the C=O stretching of carbonyl groups at 1700 cm^{-1}, the aromatic ring -C=C- stretching vibrations at 1606 and 1532 cm^{-1}. But it also presents the -C–C- deformation of the phenolic groups at 1444 cm^{-1} and the asymmetric and symmetric stretching of C–O–C etheric groups at respectively 1309 and 1182 cm^{-1}. The bands ranging from 910 to 740 cm^{-1} correspond to the C–H vibrations of the benzene rings. And more specifically, the band at 750 cm^{-1} matches the rocking vibration of methylene.

When tannic acid is methacrylated, the hydroxyl functions of TA are consumed, but the opening of the epoxide results in the grafting of a hydroxyl function. Thus, the large massif at 3300 cm^{-1} tends to sharpen because of the reduction of intramolecular hydrogen bonding rather than the consumption of hydroxyl functions, which is counterbalanced by the opening of epoxides. Methacrylated tannic acids also show the presence of a massif of peaks at around 2960–2870 cm^{-1} characteristic of the C–H stretching vibrations of CH_3 and CH_2 of glycidylmethacrylate. The intensity of the band at 1700 cm^{-1} corresponding to the C=O stretching vibration, strongly increased with the grafting of GMA due to its ester groups. The presence of GMA is confirmed by the appearance of a shoulder at 1637 cm^{-1} (C=C stretching vibration of GMA) and two peaks at 945 and 814 cm^{-1}, respectively, related to the C=C stretching and =CH_2 wagging and twisting vibrations of methacrylates. The C–O–C stretching vibration is also shifting from 1182 cm^{-1} for tannic acid to 1172 and 1168 cm^{-1} for respectively TA_{acr}5eq and TA_{acr}10eq due to the one of GMA at 1155 cm^{-1}. The IR ratio R_{acr}, defined as the ratio between the height of a characteristic band of acylates (=CH_2 twisting vibration at 814 cm^{-1}) and tannic acid (C–H vibration of the benzene ring at 870 cm^{-1}), allows to qualitatively comment on the grafting rate of the reaction. The values, gathered in Table 1, show that a higher quantity of methacrylate was indeed grafted for 10 eq. with a R_{acr} = 1.0 against 0.75 for 5 eq.

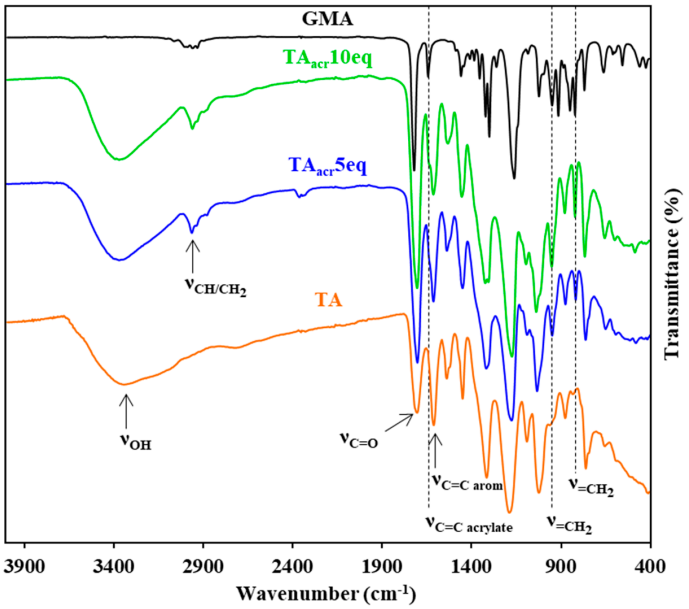

Figure 3. FTIR spectra of raw tannic acid (TA), methacrylated tannic acid 5 eq. (TA$_{acr}$5eq), methacrylated tannic acid 10 eq. (TA$_{acr}$10eq), and glycidylmethacrylate (GMA).

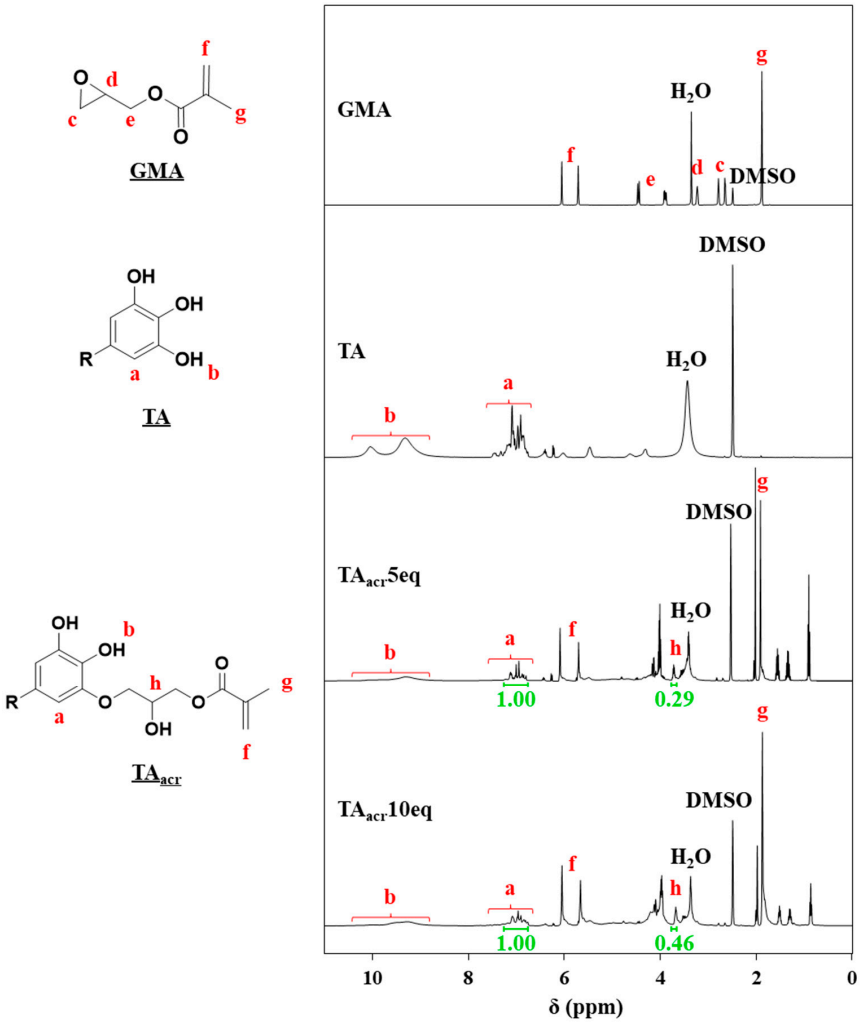

Figure 4. ^{1}H NMR spectra of glycidylmethacrylate (GMA), tannic acid (TA) and methacrylated tannic acid 10 eq. (TA$_{acr}$10eq).

Table 1. Characteristics of methacrylated tannic acids.

Sample	Racr	*DA*	Yield (%)
TAacr5eq	0.75	6.0 ± 0.6	64.8 ± 3.3
TAacr10eq	1.0	9.3 ± 1.8	87.0 ± 4.6

Grafting of GMA was also confirmed by ^{1}H NMR spectroscopy (Figure 4). The tannic acid spectrum displays two major massifs. One doublet at 10.0–9.3 ppm (b) corresponds to phenolic hydroxyl protons, and a massif at 8.0–6.7 ppm (a) corresponds to aromatic protons [50]. When GMA reacts with TA, the phenolic hydroxyl protons of the product (TA_{acr}10eq) almost disappear from the spectra. Grafting is also confirmed by the appearance of the doublet at 6.0–5.7 ppm (f) and the singlet at 1.9 ppm (g) of, respectively, the $=CH_2$ and CH_3 of the methacrylate (GMA). Finally, the appearance of the methine protons at 3.7 ppm (h) further attests the grafting and allows to calculate the substitution rate or degree of acrylation (*DA*) of the synthesized derivatives: 9.3 for TA_{acr}10eq and 6.0 for TA_{acr}5eq (Table 1). The yields of the reactions, 65 and 87%, respectively, for 5 and 10 eq. (Table 1), demonstrate that the reaction is efficient. Those results show that the reaction is quantitative and the degree of methacrylation is easily tailored.

To ensure that the grafting of methacrylate did not impart the antioxidant properties of tannic acid derivatives, the radical scavenging activity (*RSA*) of the tannins was assessed by spectrophotometry. Various techniques are described in the literature for assessing the anti-free radical activity of a compound [51,52]. They are based on the reaction between a free radical and the molecule to be tested. This radical reaction results in a change in color of the free radical used, making it possible to quantify the number of reacted radicals. The most frequently used method involves DPPH, which is a stable free radical. At room temperature, the DPPH reagent is a stable radical that strongly absorbs at 517 nm, giving a purple color to the solution. But in the presence of radical scavengers, it is neutralized, and the solution becomes colorless or pale yellow (Figure 5). Results are gathered in Figure 6. Tannic acid (TA) and its methacrylated derivatives (TA_{acr}5eq and TA_{acr}10eq) showed strong values of *RSA* (95–96%), while GMA did not exhibit strong activity (17%). Thus, the antioxidant properties of tannic acid were preserved even though methacrylate functions were grafted onto phenols.

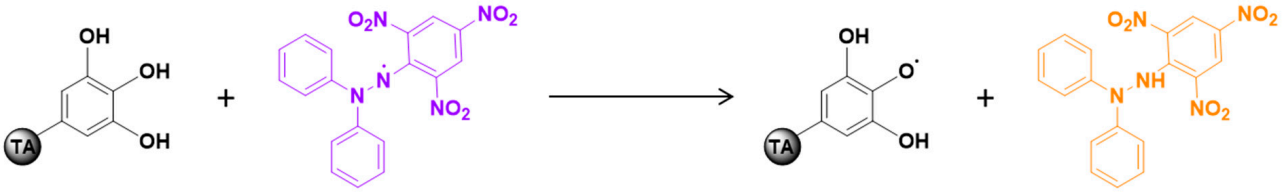

Figure 5. DPPH radical scavenging mechanism of tannic acid.

The antibacterial property of the functionalized TA was tested to ensure that the chemical modification did not alter the antimicrobial activity. The results are gathered in Figure 7. As methacrylated tannic acid is no longer soluble in aqueous media, it was dissolved in DMSO. A control of the activity of DMSO was performed to ensure that the antibacterial activity could be attributed to the methacrylated tannic acid. Results confirmed that DMSO was not fully responsible for the antibacterial activity of TA and its methacrylated derivatives, as the bacterial growth inhibition was measured at 30 and 14%, respectively, for *S. aureus* and *E. coli*. If the DMSO contribution is subtracted, as shown in Figure 7, TA and its methacrylated derivatives possess strong antibacterial activity against *S. aureus* with bacterial growth inhibition ranging from 70% at concentrations of 5 $g{\cdot}L^{-1}$. Regarding *E. coli*, the antibacterial activity is 70% for both TA derivatives at concentrations of 5 $g{\cdot}L^{-1}$ but is lower for TA, reaching 50%. The antibacterial activity is higher for TA derivatives at 5 and 0.5 $g{\cdot}L^{-1}$. In the case of *E. coli*, the antibacterial activity

of the methacrylate derivative was greater than that of tannic acid. This result could be explained by the greater solubility of the acrylate derivative in DMSO. The antibacterial activity of tannic acid is generally attributed to its ability to pass through the bacterial cell wall. Thus, the activity of tannic acid and its derivatives against Gram-positive bacteria (such as *S. aureus*) is usually stronger than against Gram-negative ones (such as *E. coli*) due to the bilayered membrane structure [21]. This was confirmed by this experiment. These promising results suggest that grafting methacrylated TA on fabrics will enable them to have antibacterial properties.

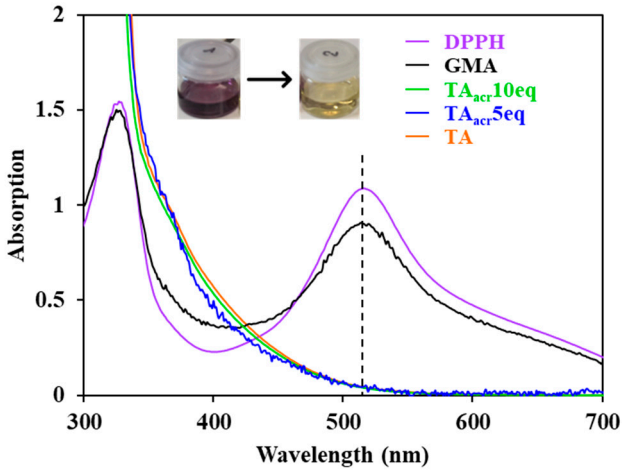

Sample	RSA (%)
GMA	17
TA_{acr}10eq	96
TA_{acr}5eq	95
TA	96

Figure 6. Absorption UV spectra of tannic acid (TA), methacrylated tannic acids (TA_{acr}5eq and TA_{acr}10eq), and GMA in the presence of DPPH.

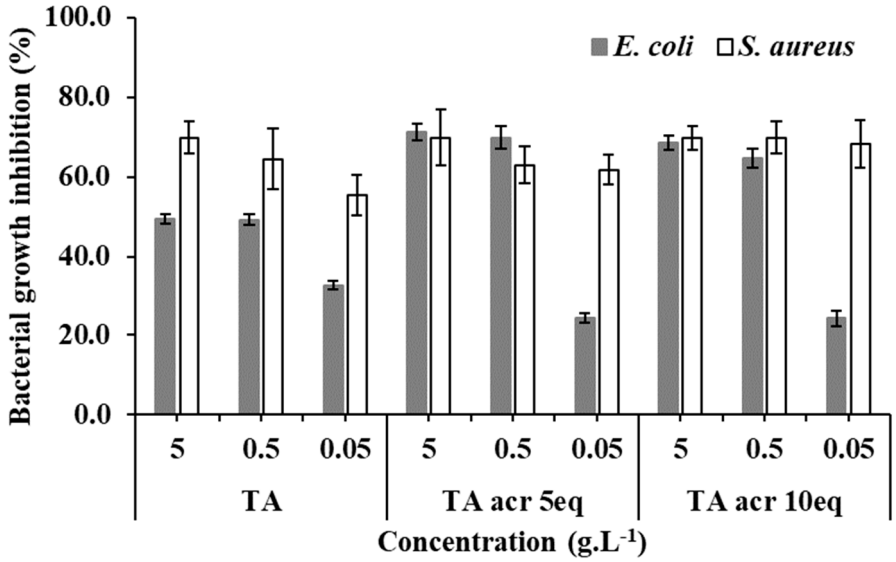

Figure 7. Antibacterial assays against *E. coli* and *S. aureus* of tannic acid (TA) and methacrylated tannic acids (TA_{acr}5eq and TA_{acr}10eq) at various concentrations after 16 h of incubation at 37 °C. Experiments were carried out in 4 replicates, and the differences are significant $p < 0.001$ for TA, both derivatives, and for the three concentrations).

3.2. Photoinduced Chemical Grafting and Polymerization of Methacrylated Tannic Acid

To overcome this challenge, chemical grafting was thus performed using a photoinitiator (DMPA) under UV irradiation. Several parameters were studied to optimize the process, such as methacrylated tannic acid concentration and degree of methacrylation, photoinitiator percentage, and number of cycles of impregnation/irradiation. The impregnation and irradiation lengths were kept constant at, respectively, 3 h and 300 s for each face. Ethanol

washing eliminated un-grafted tannic acid. Grafting/polymerization was evidenced by IR spectroscopy (Figure 8), with the appearance of peaks at 1710 cm^{-1} and 755 cm^{-1} among others, corresponding to C=O stretching vibration and methylene rocking vibration. Process optimization was followed by weight gain and IR ratio measurements; results can be found in Table 2. Significant weight gain was observed for both raw PP fibers and PP fibers coated with chitosan, attesting to the efficiency of the grafting. IR characteristic peaks of tannic acid are also more intense, compared to impregnation, resulting in higher values of R_{g1}.

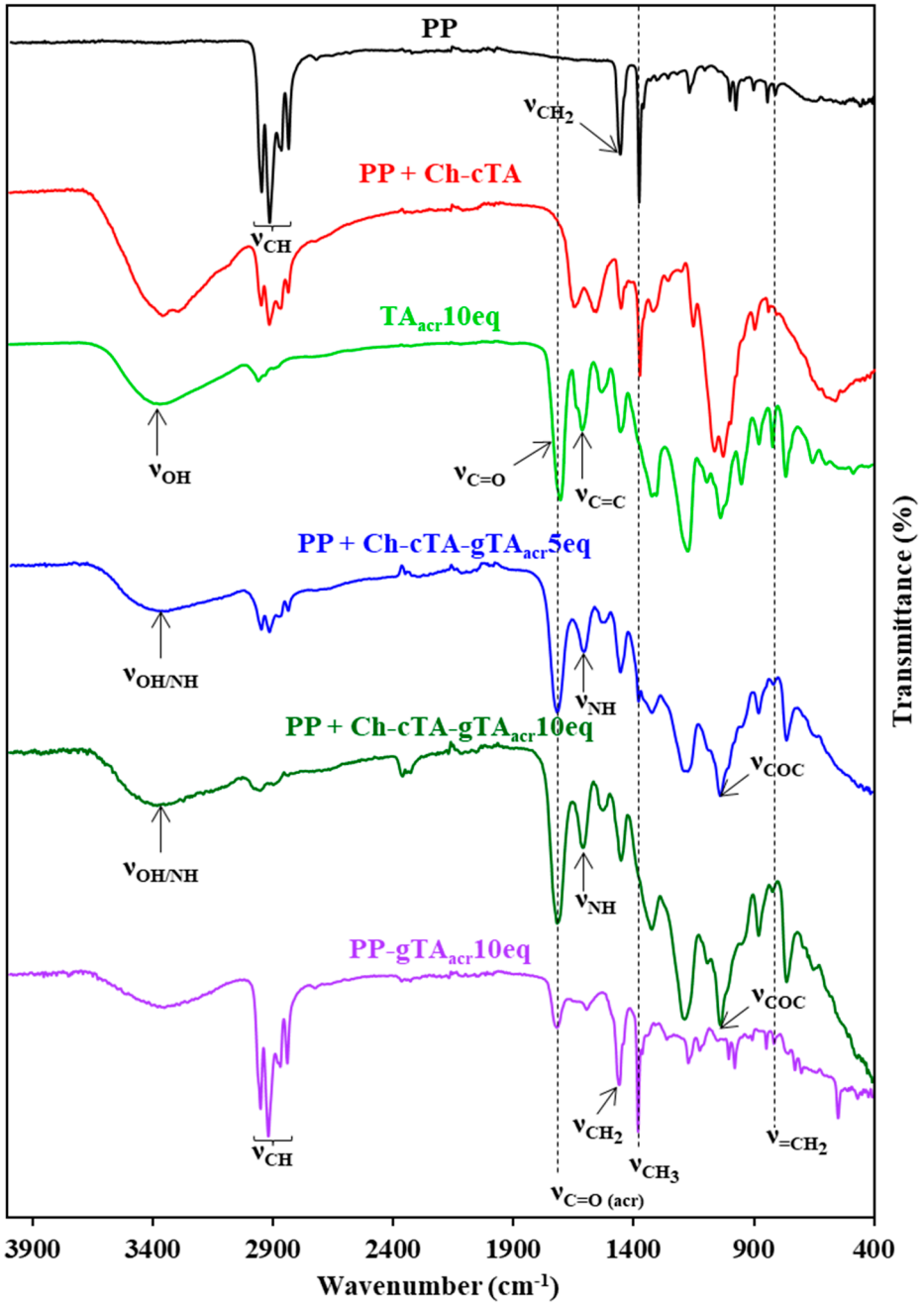

Figure 8. FTIR spectra of raw PP, PP coated with chitosan (PP + Ch-cTA), methacrylated tannic acid (TA_{acr}10eq), PP coated with chitosan grafted with TA_{acr}5eq (PP + Ch-cTA-gTA_{acr}5eq) in optimized conditions, PP coated with chitosan grafted with TA_{acr}10eq (PP + Ch-cTA-gTA_{acr}10eq) in optimized conditions, PP grafted with TA_{acr}10eq (PP-gTA_{acr}10eq) in optimized conditions.

Table 2. Characteristics of fabrics grafted with TA_{acr} in presence of a photoinitiator (DMPA) in ethanol.

Sample	Eq GMA	[TA_{acr}] (g/L)	DMPA (%)	Weight Gain (%)	R_{g1}	R_{g2}
TA_{acr}10eq	-	-	-	-	2.30	0.65
TA_{acr}5eq	-	-	-	-	2.23	0.41
PP + Ch-cTA	10	100	3	8.2 ± 2.9	[a] 0.85 ± 0.47 [b] 0.28 ± 0.12	
			3.75	7.6	[a] 1.31 ± 0.33 [b] 0.60 ± 0.19	
			5	18.4	[a] 2.01 ± 0.27 [b] 0.40 ± 0.06	0.00
		267	2.5	48.7	[a] 1.93 ± 0.38 [b] 0.88 ± 0.31	
			3.75	45.3	[a] 2.45 ± 0.16 [b] 1.34 ± 0.25	
			3.75 **	57.4	[a] 2.02 ± 0.14 [b] 2.10 ± 0.22	0.15 ± 0.3
			5	43.2	[a] 2.00 ± 0.09 [b] 1.06 ± 0.15	
			5 *	66.3	[a] 2.10 ± 0.20 [b] 2.32 ± 0.46	
			5 **	105 ± 14	[a] 1.52 ± 0.51 [b] 1.81 ± 0.48	0.09 ± 0.06
	5	100	3	2.9 ± 1.4	[a] 0.27 ± 0.11 [b] 0.27 ± 0.08	
		267	5 **	116 ± 17	[a] 1.82 ± 0.36 [b] 1.82 ± 0.31	0.11 ± 0.04
PP	10	100	3	9.1 ± 1.6	[a] 0.07 ± 0.02 [b] 0.04 ± 0.01	
		267	5 **	109 ± 17	[a] 0.20 ± 0.05 [b] 0.22 ± 0.09	0.09 ± 0.01

** 2 × 1 h 30 immersion followed by irradiation; * 2 irradiations with 2 DMPA additions; [a] 1st face irradiated; [b] 2nd face irradiated.

At a TA_{acr} concentration of 100 $g.L^{-1}$, the weight gain increases with the percentage of photoinitiator. But for higher concentrations (267 $g.L^{-1}$), photoinitiator content does not seem to influence the weight gain.

The face irradiated first, features higher values of R_{g1} than the second one. This can be explained by the fact that during the irradiation of the first face, the second face is spread on a glass plate, resulting in the loss of impregnated TA_{acr} in contact with the glass. However, when the impregnation is divided into two cycles (**) of 1 h 30 min, followed by two irradiations inversing the first face irradiated between the two cycles, the ratio difference between the two faces decreases, and R_{g1} values become less heterogeneous. Moreover, the weight gain significantly increases from 43 to 105% (for TA_{acr}10eq grafted on PP + Ch-cTA at 267 $g.L^{-1}$). Changing the first irradiated face allows to balance the loss on the glass plate. The same results were observed for TA_{acr}10eq grafted on PP and TA_{acr}5eq grafted on PP + Ch-cTA at 267 $g.L^{-1}$.

When looking at the intensity of the band at 814 cm^{-1}, attributed to the $=CH_2$ twisting vibration of methacrylated functions, a decrease appears after grafting, attesting to their consumption during the grafting/polymerization. R_{g2} indicates the consumption of methacrylate functions as well as the presence of remaining functions available for further modifications.

The optimization of the process of photoinduced grafting/polymerization resulted in two cycles of fabric impregnation in a solution of methacrylated tannic acid at 267 $g.L^{-1}$ and DMPA (photoinitiator) at 5% wt. for 1 h 30, followed by UV irradiation for 600 s

on each face. This process allows to coat inert fibers (PP) as well as fibers with reactive functions (PP + Ch-cTA).

3.3. Antioxidant Activity of Coated Fabrics

The radical scavenging activity of optimized coated fabrics was measured, and the results are presented in Figure 9. Raw fabrics were not able to discolor the DPPH solution, with *RSA* values of 3% for PP and 32% for PP coated with chitosan. This difference may be attributed to the hydroxyl and amino groups of chitosan, which can act as hydrogen donors and reduce DPPH solution [53,54]. However, when methacrylated tannic acid was grafted/polymerized onto the fabric, complete discoloration of the solution was observed for PP fabrics coated with chitosan, with an *RSA* of 95% for TA_{acr}10eq and TA_{acr}5eq. Regarding the grafting of TA_{acr}10eq onto PP fabric, a complete discoloration was also observed with an *RSA* of 94%. Thus, the treatment implemented allows for a significant antioxidant activity for both types of fabrics.

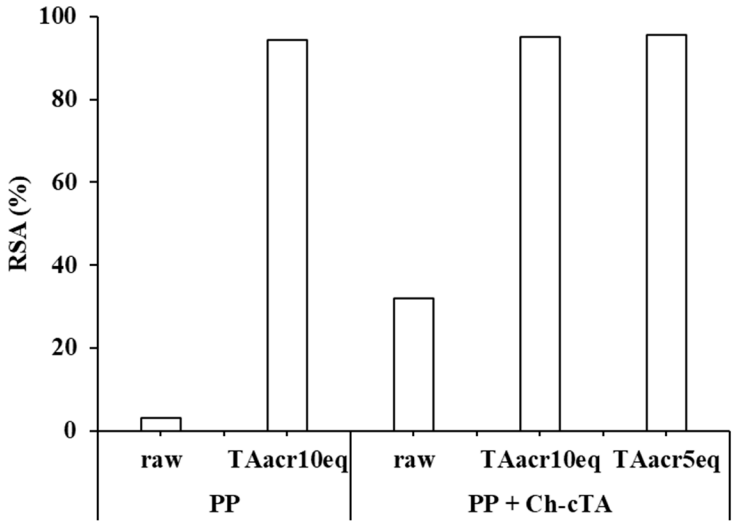

Figure 9. Radical scavenging activity of optimized fabrics photografted with TA_{acr}.

3.4. Antibacterial Activity of Coated Fabrics

Samples grafted with TA_{acr}10eq were used to assess the antibacterial activity of the coating on both types of fabrics: Raw PP and PP coated with chitosan. After 3 h of immersion at 37 °C in bacterial suspensions of *E. coli* (gram-negative) and *S. aureus* (gram-positive), fabrics were washed to desorb adhering bacteria. Those adhering bacteria were incubated for 48 h, allowing us to measure the number of colony-forming units. The results are reported in Figure 10. There was a significant antibacterial activity against *E. coli*, with bacterial adhesion ranging from 72% to 80% for grafted PP and grafted PP+chitosan. The antibacterial activity is lower with *S. aureus*, with 34% and 63% for grafted PP and grafted PP+chitosan, respectively.

From those results, we can highlight two interesting facts. The first is that grafting methacrylated tannic acid provides higher antibacterial properties against *E. coli* than *S. aureus*. This slightly contradicts the results obtained on raw TA_{acr} (Figure 7). However, it is important to note that the action of tannic acid on *S. aureus* is based on the permeability of the phenolic derivatives through the membrane. In the experiment carried out, the derivatives were covalently bound to the surface, which may explain the lower efficacy of methacrylated derivatives grafted onto the tissue compared with those obtained with TA derivatives soluble in DMSO (Figure 7). Furthermore, it can be explained by the adherence promotion of the coating. TA_{acr} are highly hydrophobic; thus, grafting TA_{acr} onto fabrics should provide a hydrophobic surface. And as *E. coli* bacteria have a more hydrophilic surface than *S. aureus*, *E. coli* bacteria will be more easily repelled than *S. aureus* [55]. The other interesting result is that PP samples coated with chitosan allowed a higher reduction

of bacterial colonization than raw PP. This can be attributed to the antibacterial properties of chitosan [36,37,56]. Thus, combining methacrylated tannic acid with chitosan increases the antibacterial properties of the coating.

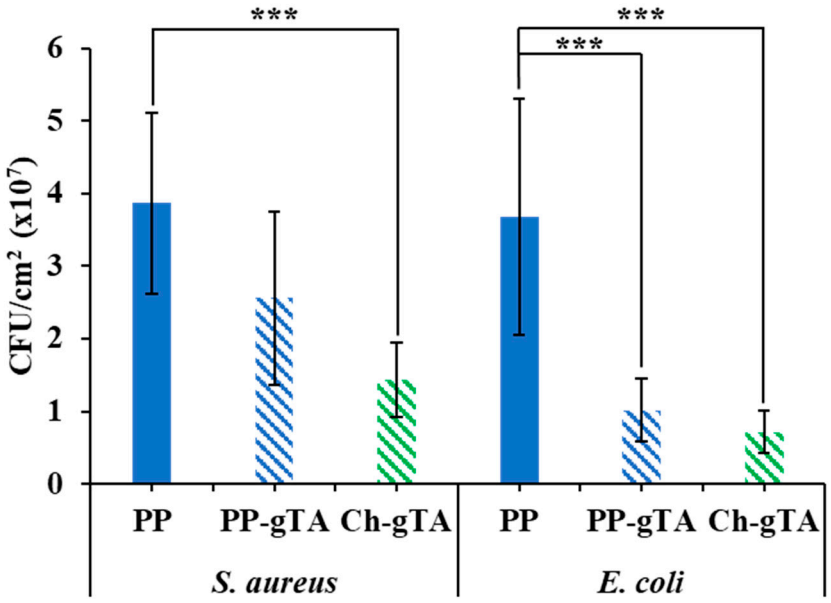

Figure 10. Antibacterial assays against *E. coli* and *S. coli* on raw PP fabrics and PP fabrics coated with chitosan both grafted with methacrylated tannic acid (TA_{acr}10eq), where *** $p < 0.001$.

Both of those results explain that PP samples coated with chitosan and grafted with TA_{acr}10eq showed significant activity against both nosocomial strains. Whereas raw PP samples grafted with TA_{acr}10eq only provided a significant reduction in bacterial colonization on *E. coli*. The combination of chitosan and methacrylated tannic acid provides the best antibacterial activity for fabrics.

4. Conclusions

In a nutshell, methacrylated tannic acid with a tunable methacrylate content was successfully synthesized. Coating with methacrylated tannic acid of inert fibers (PP) or fibers with reactive functions (PP coated with chitosan) was then achieved in a two-step process: Physical deposition and chemical grafting. Photoinduced grafting was performed to ensure strong covalent interactions and higher incorporation of TA on both types of fabrics. The process was optimized to ensure a high content of TA and coating homogeneity between the two faces by implementing two cycles of impregnation and UV irradiation. The antioxidant activity was evaluated using the DPPH test. Both fabrics showed antioxidant properties with an *RSA* of around 95%. However, regarding antibacterial activity, PP fabrics coated with chitosan showed a higher reduction in bacterial colonization than raw PP, ranging from 63% to 80% for *S. aureus* and *E. coli*, respectively. This can be attributed to the action of chitosan, which is known to possess strong antibacterial activity. The hydrophobic repellence of methacrylated tannic acid also led to a stronger action on the more hydrophilic strain, *E. coli*. This grafting process could also be transposed to any type of support since it does not mobilize any reactive functions on the surface. The synergy effect observed with chitosan suggests that this process could be advantageously transposed to sustainable polysaccharides such as cellulose mats.

Moreover, the presence of remaining methacrylate functions not involved in the reaction could enable the grafting of other active molecules, such as antimicrobial agents. The presence of chitosan could also be advantageously used to carry out post-grafting chemical modifications on the alcohol and/or amide functions of chitosan.

The results obtained are encouraging and open up interesting prospects in the context of sustainable development. Tannic acid is the simplest of the tannins and is both durable

and non-toxic. Surface grafting under irradiation is a technology aligned with the principles of green chemistry (ambient temperature, rapid kinetics, absence of solvents). The method developed can be applied to any carbon-containing surface, whether petroleum based (native and/or recyclable) or bio based. Covalent immobilization of tannic acid could also be advantageously used in membrane processes, where durability is a major parameter.

Author Contributions: Conceptualization, J.F., E.R. and L.D.; methodology, J.F., S.A.A. and V.L.; investigation, J.F., E.R. and L.D.; writing—original draft preparation, J.F.; writing—review and editing, E.R. and V.L.; supervision, E.R. All authors have read and agreed to the published version of the manuscript.

Funding: This research received no external funding.

Institutional Review Board Statement: Not applicable.

Informed Consent Statement: Not applicable.

Data Availability Statement: Data is contained within the article.

Acknowledgments: We would like to thank the French Ministry of Higher Education and Research for funding to Julie Fouilloux.

Conflicts of Interest: The authors declare no conflicts of interest.

References

1. Stegmaier, T.; Mavely, J.; Schneider, P. High-Performance and High-Functional Fibres and Textiles. In *Textiles in Sport*; Elsevier: Amsterdam, The Netherlands, 2005; pp. 89–119.
2. Karpagam, K.R.; Saranya, K.S.; Gopinathan, J.; Bhattacharyya, A. Development of Smart Clothing for Military Applications Using Thermochromic Colorants. *J. Text. Inst.* **2017**, *108*, 1122–1127. [CrossRef]
3. Shirvan, A.R.; Nouri, A. Medical Textiles. In *Advances in Functional and Protective Textiles*; Elsevier: Amsterdam, The Netherlands, 2020; pp. 291–333. ISBN 9781000514285.
4. Vandenbossche, M.; Jimenez, M.; Casetta, M.; Bellayer, S.; Beaurain, A.; Bourbigot, S.; Traisnel, M. Chitosan-Grafted Nonwoven Geotextile for Heavy Metals Sorption in Sediments. *React. Funct. Polym.* **2013**, *73*, 53–59. [CrossRef]
5. Shishoo, R. Recent Developments in Materials for Use in Protective Clothing. *Int. J. Cloth. Sci. Technol.* **2002**, *14*, 201–215. [CrossRef]
6. Kenawy, E.R.; Bowlin, G.L.; Mansfield, K.; Layman, J.; Simpson, D.G.; Sanders, E.H.; Wnek, G.E. Release of Tetracycline Hydrochloride from Electrospun Poly(Ethylene-Co-Vinylacetate), Poly(Lactic Acid), and a Blend. *J. Control. Release* **2002**, *81*, 57–64. [CrossRef] [PubMed]
7. Rujitanaroj, P.-o.; Pimpha, N.; Supaphol, P. Wound-Dressing Materials with Antibacterial Activity from Electrospun Gelatin Fiber Mats Containing Silver Nanoparticles. *Polymer* **2008**, *49*, 4723–4732. [CrossRef]
8. He, W.; Yong, T.; Teo, W.E.; Ma, Z.; Ramakrishna, S. Fabrication and Endothelialization of Collagen-Blended Biodegradable Polymer Nanofibers: Potential Vascular Graft for Blood Vessel Tissue Engineering. *Tissue Eng.* **2005**, *11*, 1574–1588. [CrossRef] [PubMed]
9. Baldwin, A.; Booth, B.W. Biomedical Applications of Tannic Acid. *J. Biomater. Appl.* **2022**, *36*, 1503–1523. [CrossRef]
10. Kim, H.; Panda, P.K.; Sadeghi, K.; Lee, S.; Chung, C.; Park, Y.; Park, J.; Seo, J. Facile Thermal and Hydrolytic Conversion of Tannic Acid: Enhancement of Antimicrobial Activity and Biocompatibility for Biomedical Applications. *Mater. Chem. Phys.* **2022**, *285*, 126141. [CrossRef]
11. Kaczmarek-Szczepańska, B.; Sionkowska, M.M.; Mazur, O.; Świątczak, J.; Brzezinska, M.S. The Role of Microorganisms in Biodegradation of Chitosan/Tannic Acid Materials. *Int. J. Biol. Macromol.* **2021**, *184*, 584–592. [CrossRef]
12. Yu, G.; Dan, N.; Dan, W.; Chen, Y. Wearable Tissue Adhesive Ternary Hydrogel of N-(2-Hydroxyl) Propyl-3-Trimethyl Ammonium Chitosan, Tannic Acid, and Polyacrylamide. *Ind. Eng. Chem. Res.* **2022**, *61*, 5502–5513. [CrossRef]
13. Hu, N.; Qin, H.; Chen, X.; Huang, Y.; Xu, J. Tannic Acid Assisted Metal—Chelate Interphase toward Highly Stable Zn Metal Anodes in Rechargeable Aqueous Zinc-Ion Batteries. *Front. Chem.* **2022**, *10*, 981623. [CrossRef] [PubMed]
14. Huang, X.; Wu, H.; Liao, X.; Shi, B. One-Step, Size-Controlled Synthesis of Gold Nanoparticles at Room Temperature Using Plant Tannin. *Green Chem.* **2010**, *12*, 395–399. [CrossRef]
15. Fan, H.; Wang, L.; Feng, X.; Bu, Y.; Wu, D.; Jin, Z. Supramolecular Hydrogel Formation Based on Tannic Acid. *Macromolecules* **2017**, *50*, 666–676. [CrossRef]
16. Akiyama, H.; Fujii, K.; Yamasaki, O.; Oono, T.; Iwatsuki, K. Antibacterial Action of Several Tannins against *Staphylococcus aureus*. *J. Antimicrob. Chemother.* **2001**, *48*, 487–491. [CrossRef] [PubMed]
17. Sathishkumar, G.; Gopinath, K.; Zhang, K.; Kang, E.T.; Xu, L.; Yu, Y. Recent Progress in Tannic Acid-Driven Antibacterial/Antifouling Surface Coating Strategies. *J. Mater. Chem. B* **2022**, *10*, 2296–2315. [CrossRef]

18. Gülçin, I.; Huyut, Z.; Elmastaş, M.; Aboul-Enein, H.Y. Radical Scavenging and Antioxidant Activity of Tannic Acid. *Arab. J. Chem.* **2010**, *3*, 43–53. [CrossRef]
19. Sahiner, N.; Sengel, S.B. Tannic Acid Decorated Poly(Methacrylic Acid) Micro and Nanoparticles with Controllable Tannic Acid Release and Antioxidant Properties. *Colloids Surf. A Physicochem. Eng. Asp.* **2016**, *508*, 30–38. [CrossRef]
20. Widsten, P.; Cruz, C.D.; Fletcher, G.C.; Pajak, M.A.; McGhie, T.K. Tannins and Extracts of Fruit Byproducts: Antibacterial Activity against Foodborne Bacteria and Antioxidant Capacity. *J. Agric. Food Chem.* **2014**, *62*, 11146–11156. [CrossRef]
21. Kaczmarek, B. Tannic Acid with Antiviral and Antibacterial Activity as a Promising Component of Biomaterials-A Minireview. *Materials* **2020**, *13*, 3224. [CrossRef]
22. Konowalchuk, J.; Speirs, J.I. Antiviral Activity of Fruit Extracts. *J. Food Sci.* **1976**, *41*, 1013–1017. [CrossRef]
23. Ninan, N.; Forget, A.; Shastri, V.P.; Voelcker, N.H.; Blencowe, A. Antibacterial and Anti-Inflammatory PH-Responsive Tannic Acid-Carboxylated Agarose Composite Hydrogels for Wound Healing. *ACS Appl. Mater. Interfaces* **2016**, *8*, 28511–28521. [CrossRef] [PubMed]
24. Yeo, J.; Lee, J.; Yoon, S.; Kim, W.J. Tannic Acid-Based Nanogel as an Efficient Anti-Inflammatory Agent. *Biomater. Sci.* **2020**, *8*, 1148–1159. [CrossRef] [PubMed]
25. Lobo, V.; Patil, A.; Phatak, A.; Chandra, N. Free Radicals, Antioxidants and Functional Foods: Impact on Human Health. *Pharmacogn. Rev.* **2010**, *4*, 118–126. [CrossRef] [PubMed]
26. Deng, L.; Du, C.; Song, P.; Chen, T.; Rui, S.; Armstrong, D.G.; Deng, W. The Role of Oxidative Stress and Antioxidants in Diabetic Wound Healing. *Oxid. Med. Cell Longev.* **2021**, *2021*, 8852759. [CrossRef] [PubMed]
27. Zemljič, L.F.; Volmajer, J.; Ristić, T.; Bracic, M.; Sauperl, O.; Kreže, T. Antimicrobial and Antioxidant Functionalization of Viscose Fabric Using Chitosan–Curcumin Formulations. *Text. Res. J.* **2014**, *84*, 819–830. [CrossRef]
28. Gulati, R.; Sharma, S.; Sharma, R.K. Antimicrobial Textile: Recent Developments and Functional Perspective. *Polym. Bull.* **2022**, *79*, 5747–5771. [CrossRef] [PubMed]
29. Zhang, W.; Yang, Z.Y.; Tang, R.C.; Guan, J.P.; Qiao, Y.F. Application of Tannic Acid and Ferrous Ion Complex as Eco-Friendly Flame Retardant and Antibacterial Agents for Silk. *J. Clean. Prod.* **2020**, *250*, 119545. [CrossRef]
30. Zhang, W.; Yang, Z.Y.; Cheng, X.W.; Tang, R.C.; Qiao, Y.F. Adsorption, Antibacterial and Antioxidant Properties of Tannic Acid on Silk Fiber. *Polymers* **2019**, *11*, 970. [CrossRef] [PubMed]
31. Dai, H.; Chen, Y.; Zhang, S.; Feng, X.; Cui, B.; Ma, L.; Zhang, Y. Enhanced Interface Properties and Stability of Lignocellulose Nanocrystals Stabilized Pickering Emulsions: The Leading Role of Tannic Acid. *J. Agric. Food Chem.* **2021**, *69*, 14650–14661. [CrossRef] [PubMed]
32. Perelshtein, I.; Ruderman, E.; Francesko, A.; Fernandes, M.M.; Tzanov, T.; Gedanken, A. Tannic Acid NP—Synthesis and Immobilization onto a Solid Surface in a One-Step Process and Their Antibacterial and Anti-Inflammatory Properties. *Ultrason. Sonochem.* **2014**, *21*, 1916–1920. [CrossRef]
33. Espinosa-Jiménez, M.; Giménez-Martín, E.; Ontiveros-Ortega, A. Effect of Tannic Acid on the ζ Potential, Sorption, and Surface Free Energy in the Process of Dyeing of Leacril with a Cationic Dye. *J. Colloid. Interface Sci.* **1998**, *207*, 170–179. [CrossRef]
34. Gao, C.; Petrova, S.P.; Edgar, K.J. Chlorination of Hydroxyethyl Cellulose Enables Selective Functionalization. *Cellulose* **2024**, *31*, 1481–1495. [CrossRef]
35. Gao, C.; Liu, S.; Edgar, K.J. Regioselective Chlorination of Cellulose Esters by Methanesulfonyl Chloride. *Carbohydr. Polym.* **2018**, *193*, 108–118. [CrossRef] [PubMed]
36. Goy, R.C.; Morais, S.T.B.; Assis, O.B.G. Evaluation of the Antimicrobial Activity of Chitosan and Its Quaternized Derivative on E. Coli and S. Aureus Growth. *Rev. Bras. De Farmacogn.* **2016**, *26*, 122–127. [CrossRef]
37. Li, J.; Tian, X.; Hua, T.; Fu, J.; Koo, M.; Chan, W.; Poon, T. Chitosan Natural Polymer Material for Improving Antibacterial Properties of Textiles. *ACS Appl. Bio Mater.* **2021**, *4*, 4014–4038. [CrossRef] [PubMed]
38. Wang, H.; Qian, J.; Ding, F. Emerging Chitosan-Based Films for Food Packaging Applications. *J. Agric. Food Chem.* **2018**, *66*, 395–413. [CrossRef]
39. Wang, L.; Liu, F.; Jiang, Y.; Chai, Z.; Li, P.; Cheng, Y.; Jing, H.; Leng, X. Synergistic Antimicrobial Activities of Natural Essential Oils with Chitosan Films. *J. Agric. Food Chem.* **2011**, *59*, 12411–12419. [CrossRef]
40. Deng, L.; Taxipalati, M.; Zhang, A.; Que, F.; Wei, H.; Feng, F.; Zhang, H. Electrospun Chitosan/Poly(Ethylene Oxide)/Lauric Arginate Nanofibrous Film with Enhanced Antimicrobial Activity. *J. Agric. Food Chem.* **2018**, *66*, 6219–6226. [CrossRef]
41. Wang, Y.; Li, J.; Li, B. Nature-Inspired One-Step Green Procedure for Enhancing the Antibacterial and Antioxidant Behavior of a Chitin Film: Controlled Interfacial Assembly of Tannic Acid onto a Chitin Film. *J. Agric. Food Chem.* **2016**, *64*, 5736–5741. [CrossRef]
42. Fouilloux, J.; Abbad-Andaloussi, S.; Langlois, V.; Dammak, L.; Renard, E. Green Physical Modification of Polypropylene Fabrics by Cross-Linking Chitosan with Tannic Acid and Postmodification by Quaternary Ammonium Grafting to Improve Antibacterial Activity. *ACS Appl. Bio Mater.* **2023**. [CrossRef]
43. Glaive, A.S.; Modjinou, T.; Versace, D.L.; Abbad-Andaloussi, S.; Dubot, P.; Langlois, V.; Renard, E. Design of Antibacterial and Sustainable Antioxidant Networks Based on Plant Phenolic Derivatives Used as Delivery System of Carvacrol or Tannic Acid. *ACS Sustain. Chem. Eng.* **2017**, *5*, 2320–2329. [CrossRef]
44. Modjinou, T.; Versace, D.L.; Abbad-Andallousi, S.; Bousserrhine, N.; Babinot, J.; Langlois, V.; Renard, E. Antibacterial Networks Based on Isosorbide and Linalool by Photoinitiated Process. *ACS Sustain. Chem. Eng.* **2015**, *3*, 1094–1100. [CrossRef]

45. Jing, W.; Xiaolan, C.; Yu, C.; Feng, Q.; Haifeng, Y. Pharmacological Effects and Mechanisms of Tannic Acid. *Biomed. Pharmacother.* **2022**, *154*, 113561. [CrossRef]
46. Le, S.D.; Nishimura, S.; Ebitani, K. Direct Esterification of Succinic Acid with Phenol Using Zeolite Beta Catalyst. *Catal. Commun.* **2019**, *122*, 20–23. [CrossRef]
47. Cazorla, C.; Pfordt, E.; Duclos, M.; Métay, E.; Lemaire, M. O-Alkylation of Phenol Derivatives via a Nucleophilic Substitution. *Green Chem.* **2011**, *13*, 2482–2488. [CrossRef]
48. Chen, Z.; Zeng, H.; Girard, S.A.; Wang, F.; Chen, N.; Li, C. Formal Direct Cross-Coupling of Phenols with Amines. *Angew. Chem.* **2015**, *54*, 14487–14491. [CrossRef] [PubMed]
49. Liu, R.; Zhu, J.; Luo, J.; Liu, X. Synthesis and Application of Novel UV-Curable Hyperbranched Methacrylates from Renewable Natural Tannic Acid. *Prog. Org. Coat.* **2014**, *77*, 30–37. [CrossRef]
50. Cuthbert, J.; Yerneni, S.S.; Sun, M.; Fu, T.; Matyjaszewski, K. Degradable Polymer Stars Based on Tannic Acid Cores by ATRP. *Polymers* **2019**, *11*, 752. [CrossRef]
51. Basak, S.; Mukherjee, I.; Das, T.K. Injectable Biocompatible RAFT Mediated Nitroxide Nanogels: A Robust ROS-Reduction Antioxidant Approach. *Colloids Surf. B Biointerfaces* **2024**, *236*, 113790. [CrossRef]
52. Han, B.; Chen, P.; Guo, J.; Yu, H.; Zhong, S.; Li, D.; Liu, C.; Feng, Z.; Jiang, B. A Novel Intelligent Indicator Film: Preparation, Characterization, and Application. *Molecules* **2023**, *28*, 3384. [CrossRef]
53. Jung, J.; Zhao, Y. Comparison in Antioxidant Action between α-Chitosan and β-Chitosan at a Wide Range of Molecular Weight and Chitosan Concentration. *Bioorg. Med. Chem.* **2012**, *20*, 2905–2911. [CrossRef] [PubMed]
54. Wan, A.; Xu, Q.; Sun, Y.; Li, H. Antioxidant Activity of High Molecular Weight Chitosan and N,O-Quaternized Chitosans. *J. Agric. Food Chem.* **2013**, *61*, 6921–6928. [CrossRef]
55. Mirani, Z.A.; Fatima, A.; Urooj, S.; Aziz, M.; Khan, M.N.; Abbas, T. Relationship of Cell Surface Hydrophobicity with Biofilm Formation and Growth Rate: A Study on *Pseudomonas aeruginosa*, *Staphylococcus aureus*, and *Escherichia coli*. *Iran J. Basic Med. Sci.* **2018**, *21*, 760–769. [CrossRef]
56. Li, J.; Zhuang, S. Antibacterial Activity of Chitosan and Its Derivatives and Their Interaction Mechanism with Bacteria: Current State and Perspectives. *Eur. Polym. J.* **2020**, *138*, 109984. [CrossRef]